EME-Net: A U-net-based Indoor EMF Exposure Map Reconstruction Method

Mohammed Mallik*, Sofiane Kharbech†, Taghrid Mazloum‡, Shanshan Wang‡, Joe Wiart‡,
Davy P. Gaillot* and Laurent Clavier*†
* Univ. Lille, CNRS, Centrale Lille, Univ. Polytechnique Hauts-de-France,
UMR 8520 - IEMN - Institut d'Electronique de Microélectronique et de Nanotechnologie, F-59000 Lille, France
† IMT Nord Europe, Centre for Digital Systems, Lille, France
‡ Chaire C2M, LTCI, Télécom Paris, Institut Polytechnique de Paris, Palaiseau, France
mohammed.mallik.etu@univ-lille.fr

***Abstract*—In wireless communication systems, in order to respond to the perception of risks related to electromagnetic field exposure and allocate radio resources, the estimation of the received power and exposure map is an essential task and a challenge. This paper proposes an algorithm for estimating electromagnetic field exposure maps using U-net architecture based on convolutional neural networks. The power map estimation is transformed into an image reconstruction task by image color mapping, where every pixel value of the image represents received power intensity. The designed model learns wireless signal propagation characteristics in a realistic indoor environment while considering various positions of the Wi-Fi access points. Results show that indoor propagation phenomena and environment models can be learned from data producing an accurate power map to measure the electromagnetic field.**

***Index Terms*—EMF exposure, convolutional neural network, image reconstruction, optimization.**

I. Introduction

With the increasing growth of wireless communication systems, evaluating the radiofrequency electromagnetic field (RF-EMF) is worthy of further investigation. Wi-Fi communication systems are widely used, especially in indoor environments. Due to the extensive Wi-Fi deployment, the assessment of health risk perception of the RF-EMF and radio resource allocation is essential [1], [2]. Multiple studies were conducted to measure the exposure level for the RF-EMF sources radiating within the frequency range 10 MHz to 6 GHz, such as mobile radio networks, Wi-Fi, RF identification tagging systems, Wireless Local Area Network, radio and television broadcasting, and cordless phones (DECT) [3]. Sensor networks and on-site measurements are significant, but they are localized systems causing EMF exposure monitoring at limited locations. For an indoor environment, locations of Wi-Fi access points in a building may depend on features like the building architecture, furniture, or room size. Therefore it is necessary to build a power map to assess RF-EMF exposure considering these related aspects.

In [4], considering urban cognitive radio networks, authors estimate the power spectrum map using a Generative Adversarial Network (GAN) [5], [6] based on convolutional neural networks (CNN). Frequencies of 25 MHz and 75 MHz are used and users are assumed to be uniformly distributed. The power spectrum is calculated as a deep learning regression task, then mapped to a color spectrum. These power spectrum maps were fed into a GAN model based on autoencoders analogy as an image reconstruction task. In the estimated power spectrum maps (PSMs), authors were limited to the inverse polynomial law model to represent propagation phenomena. While in the present paper, to accurately represent the indoor propagation characteristics, we additionally considered specific parameters such as effects of building walls, materials, brick, partitions, etc.

In this work, RF-EMF exposure is assessed to Wi-Fi access points at different locations in a realistic indoor environment, where channel frequencies vary from 2.412 GHz to 2.472 GHz. This is achieved using a CNN-based architecture embedding the popular U-net [7] model used for biomedical image segmentation. The introduced reconstruction model is referred to as Exposure Map Estimation Network (EME-Net). The pixel color in the reference power map image of the indoor environment represents the power intensity. The EME-Net model is designed to learn and then predict the indoor wireless propagation characteristics such as reflection, diffraction, shadowing, the effect of building walls, and materials.

The paper is organized as follows. In Section II, we describe the proposed U-net-based RF-EMF exposure power map estimation algorithm. Experimental findings are presented and discussed in Section III. At the end, Section IV concludes the paper.

II. The EME-net model

A. Sensor Measurement Exposure Power Map

Since estimating the EMF exposure map is essentially an image reconstruction task, the EME-Net model's input is an image as a three-dimensional matrix. The dimensions are the height, width, and color channel. An image is built by combining four channels, i.e., red, green, blue, and alpha. In simple words, a channel refers to color intensity and color in the image. In the original U-net model, input image channel depth was set to one to predict a single-channel mask. In contrast, a three-dimensional image tensor with channel depth four is utilized for our method to reconstruct the output image. Image properties are described in Table I. The color intensity

of each pixel of the input image represents the sensor measured value at a corresponding location, making the input sensor measurement map.

TABLE I: Properties of the image representing the EMF map.

Dimension	3
1st dimension	height - 267
2nd dimension	width - 665
3rd dimension	channel
Channel depth	4
Channel 1	red
Channel 2	green
Channel 3	blue
Channel 4	alpha

B. EME-Net: Exposure Map Estimation Network

The exposure map estimator system, labeled EME-Net, is composed of two modules in Figure 1. The first module is the reduction module and consists of convolutional, max-pooling, and dropout layers that extract the features of the input images by downsampling. The second module is the expansion module: a symmetric expanding path consisting of transposed convolutional layers upsampling the feature matrix. The architecture follows the structure of auto-encoders. The model is designed to capture the information from the training dataset, learn more complex wireless propagation features of the target area, and reconstruct the power map for exposure measurement.

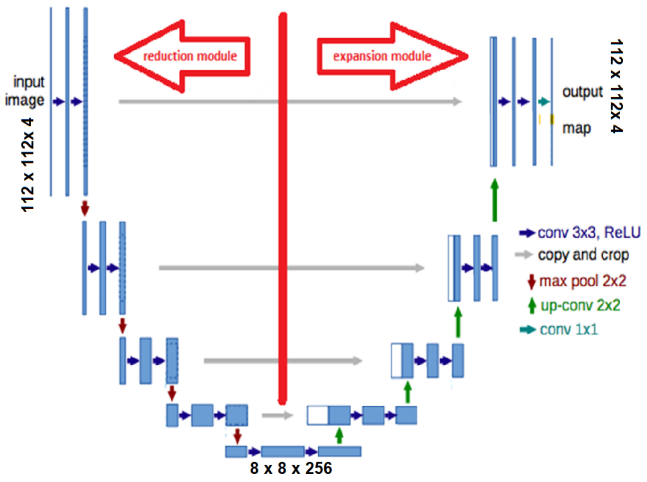

Fig. 1: The EME-Net model architecture.

Every layer of the expansion module uses skip connections by concatenating the output of the convolutional layers and the feature extraction layer. This is processed through the contraction module of the same level. The contraction module of the proposed EME-Net model encodes and learns features extracted from the input measurement map while keeping the spatial information of the input image. The proposed model can then generate the RF-EMF exposure power map from the input sensor measurement one. The explanations of the modules are following.

1) Reduction Module: For the EME-Net model, the input layer takes a three-dimensional sensor measurement image. The reduction module is a chain of blocks, each of them is composed of

- Two consecutive convolutional layers with kernel size 3×3, a stride of 1. The input layer takes a three-dimensional sensor measurement image, i.e., tensors with size $112 \times 112 \times 4$. This increases the channel number of the feature map and results in new dimensions with 16 channels.
- The employed activation function is the rectified linear unit (ReLU). Taking only positive values after convolution serves to overcome the vanishing gradient problem during the backpropagation process while updating the model weights.
- Previous layers are ended with a max-pooling layer. The largest value in each patch of each feature map is taken in this layer, downsampling the feature map. This results in new dimensions: $64 \times 64 \times 16$.

Layers in the first block are repeated in the reduction module, where the feature map size gradually reduces while the depth or channel number increases to $8 \times 8 \times 256$.

2) Expansion Module: In the expansion module, five symmetric blocks of the reduction module are used with a transposed convolutional layer for upsampling. Layers parameters are set so that the height and width of the feature map are doubled, whereas the depth (number of channels) is halved.

Two successive convolutions are applied to learn more definite features from the feature map. The proposed EME-Net model architecture is symmetric U-shaped and has five blocks on each module. On a high level, it can be illustrated as in Fig. 2.

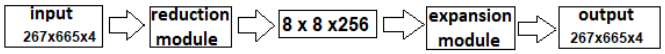

Fig. 2: EME-Net model at a high level.

Next, we compare three U-net-based architectures, namely EME-Net with 2 blocks, EME-Net with 3 blocks, and EME-Net with 5 blocks on both modules (i.e., reduction and expansion). Then, the best model is selected for testing.

C. Training and Testing the Model

The input data are the sensor measurement map images and the model output are the RF-EMF exposure map images.

The RF-EMF exposure power map estimation is an image reconstruction task that could be treated as a regression problem. We minimized the regression loss using the L_2 mean squared error function during both training and validation to optimize the parameters and update the proposed model weights.

The reconstructed map images are compared with the reference RF-EMF maps during the test phase to investigate the model performance. The test result yields the reconstruction performance for a lower to a higher number of sensor measurement locations. Visual observations of some samples of the reconstructed power map will also be provided.

D. Evaluation Metrics

To evaluate the model performance, the structural similarity index (SSIM) [8] and the peak signal-to-noise ratio (PSNR) are calculated based on the reconstructed map and the reference map. SSIM models the perceived change in the structural information of the image, giving values between -1 and 1, where 1 indicates perfect similarity. PSNR measures the ratio between the highest of the maximum pixel intensity to the power of the distortion.

III. Simulation Results

This section describes the indoor propagation environment, introduces the simulation parameters, and discusses the EMF map reconstruction results.

A. The Environment Model

For computer simulations, we consider a customized version of the environment WINNER-II A1 [9]. It represents a typical multi-room office environment where the floor area is 2100 m^2, room dimensions are 10 m $\times$ 10 m $\times$ 3 m, and the corridor has the dimensions 70 m $\times$ 10 m $\times$ 3 m. Windows are located on the north and south side of the office environment. Each room has a wooden door, and the walls are constructed with plaster with a thickness of 10cm. The ceiling and floor are made using reinforced concrete. The indoor office model layout is illustrated in Fig. 3. Materials used to construct the rooms and their properties are given in Table II. They are implemented in 'PyLayers' for the simulations. For training the model, 5 Wi-Fi access points are considered with different location scenarios while keeping two of them in the corridor and three in the rooms. 'PyLayers' is an open-source radio-channel wave propagation simulation tool [10]. Using 'PyLayers', we simulate the received power maps in a dense environment; then, we employ them as reference maps. Figure 4, gives two examples of reference exposure maps with different Wi-Fi access points locations'. Five pixels in each room and 26 pixels in the corridor, 96 pixels were taken from the reference map to generate the sensor measurement maps. Sensor measurement locations as the incomplete image are shown in figure 5. We consider 15, 30, 50, 70, 90, and 115 pixels taken from the reference map images for the test sets. It is worth noting that, for the most optimistic scenario, i.e., when 115 measures or pixels are considered, we cover less than 1% of the reference image area.

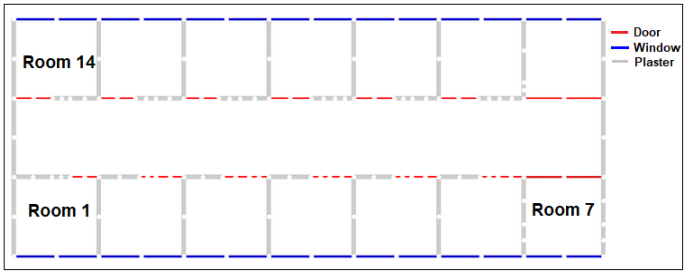

Fig. 3: Layout of the indoor scenario.

Description	Wall	Air	Ceiling	Floor	Door
Material	Plaster	Air	Reinforced concrete	Reinforced concrete	Wood
Relative permeability μ_r	$1+0j$	$1+0j$	$1+0j$	$1+0j$	$1+0j$
Relative permittivity ε_r	$8.0+0j$	$1+0j$	$8.09+0j$	$8.09+0j$	$8.3+0.02j$
Sigma conductivity s/m	0.308	0	0	0	0
Thickness in cm	10	2	10	10	5
Manning's roughness	0.0	0.0	0.012	0.0	0.0

TABLE II: Properties of the environment materials.

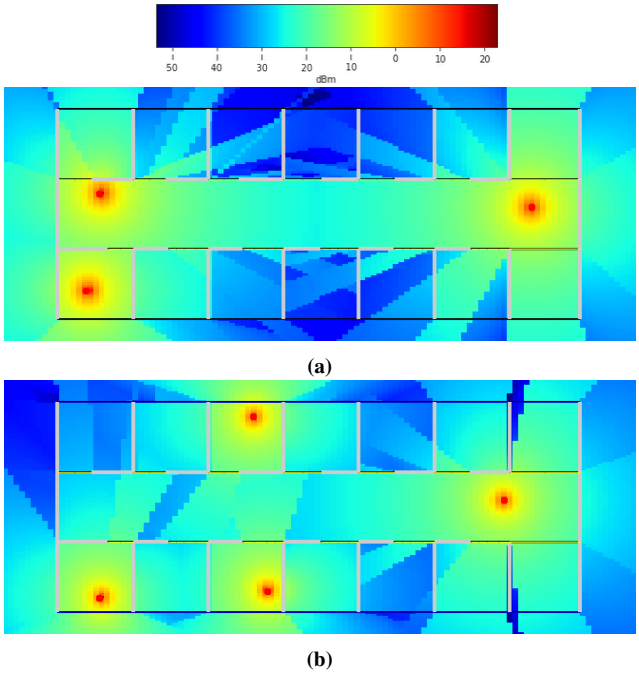

(a)

(b)

Fig. 4: RF-EMF exposure reference map

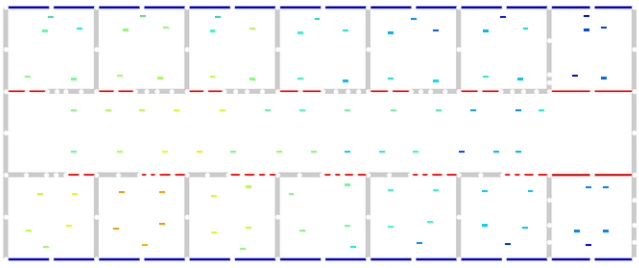

Fig. 5: Input sensor measurement map with 96 pixels from the reference map.

The Wi-Fi hotspots are omnidirectional with orthogonal and parallel polarization. Generating the EMF exposure maps considers the multi-wall and multi-frequency home environment path loss model [11]. The path loss is calculated taking into account that the direct line between Tx and Rx crosses several kinds and amounts of walls added to the free space log-distance path loss:

$$PL(d)[dB] = PL_0(d_0) + 20log_{10}(d/d_0) + \sum_{i=1}^{M} k_i L_i + X\sigma$$

where $PL(d)$ is the path loss at a Tx - Rx distance equal to PL_0 at a reference distance d_0 equal to 1m is the path loss, k_i is the number of walls of type i crossed by the line-of-sight, the total number of different kinds of wall is M, L_i is the penetration loss of wall type i, and is X_σ is a zero-mean gaussian random variable with a standard deviation σ. The value for $PL_0(d_0)$ and X_σ for a Wi-Fi radio technology at frequency band $2.4 - 2.5GHz$ are $27.75dB$ and $5.94dB$ respectively.

The core objective of this study is to investigate whether the proposed EME-Net model could learn accurate propagation characteristics with the given environment architecture. Reference maps are generated using the features of propagation such as the multi-wall loss, the type of material used to construct the wall, the wall penetration loss, the relative permeability and permittivity, the conductivity, and the thickness of walls.

B. The Results

We evaluate the proposed EME-Net through three different configurations by varying the number of blocks of the convolutional layers in both reduction and expansion modules. These three configurations were trained and evaluated on the same datasets. For the input training samples, 96 pixels as measurement locations are used. Training setup, description of the derived three models and losses are depicted in tables III and IV respectively.

Parameters	Value
Total number of images	12660
Input samples	10128
Validation set	1266
Test set	100
Optimizer	ADAM -Adaptive Moment Algorithm
Learning rate	1×10^{-4}
Batch size	2
Decay rate	1×10^{-6}
Epochs	12

TABLE III: Training parameters.

Model (or configuration)	Trainable parameters	loss
EME-Net 2 blocks	61400	0.0183
EME-Net 3 blocks	114800	0.0102
EME-Net 5 blocks	**1942428**	**0.0017**

TABLE IV: Total number of parameters for each reconstruction model and training loss.

Following the training of the EME-Net derived models (EME-Net-2 blocks, EME-Net-3 blocks, and EME-Net-5 blocks), the one with the minimum loss was chosen as the best performing model. Results shown in Table IV.

The best model performance was investigated by increasing the number of measurement points. This is done by taking 15, 30, 50, 90, 115 pixels as measurement points from the reference image.

Figure 8 illustrates the reconstructed maps using the proposed EME-Net model based on test sets containing 15, 50, 90 pixels as measurement points.

Figure 6 shows the SSIM value of reference and reconstructed images increases with the number of measurements in the input image. When 15 measurements are fed in the model, the reconstructed images have lower SSIM; while increasing the number of measurement points, the SSIM value gradually increases. SSIM value lower means dissimilarity between reference and reconstructed images.

Figure 7 presents both averages of SSIM and PSNR increase together with the number of measurement points. About the slight downfall of the average SSIM at 90 measurements, this effect is due to the use of raw pixels intensities globally.Same trend indicating that the reconstruction process is coherent with respect to similarity and image quality.

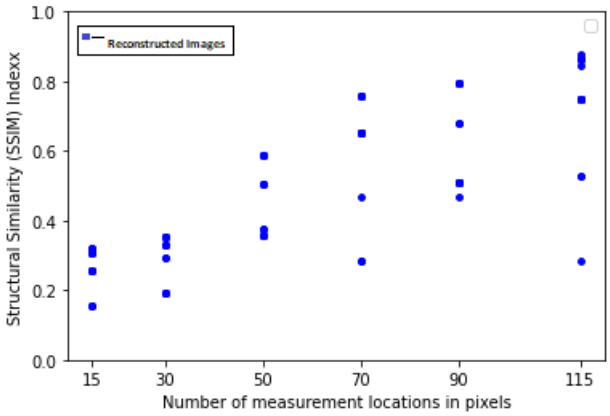

Fig. 6: SSIM - reference and reconstructed images.

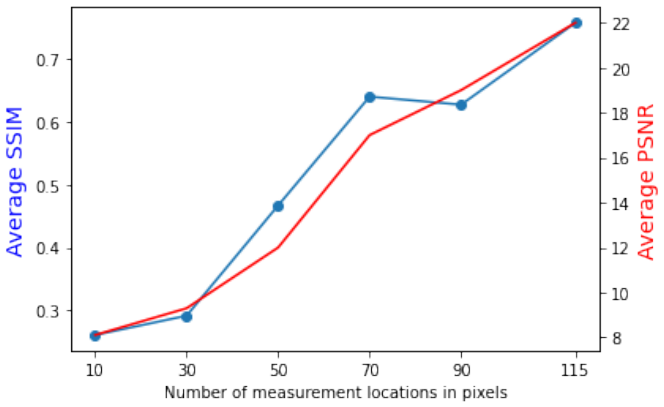

Fig. 7: Reference Vs. Reconstructed - average SSIM and PSNR.

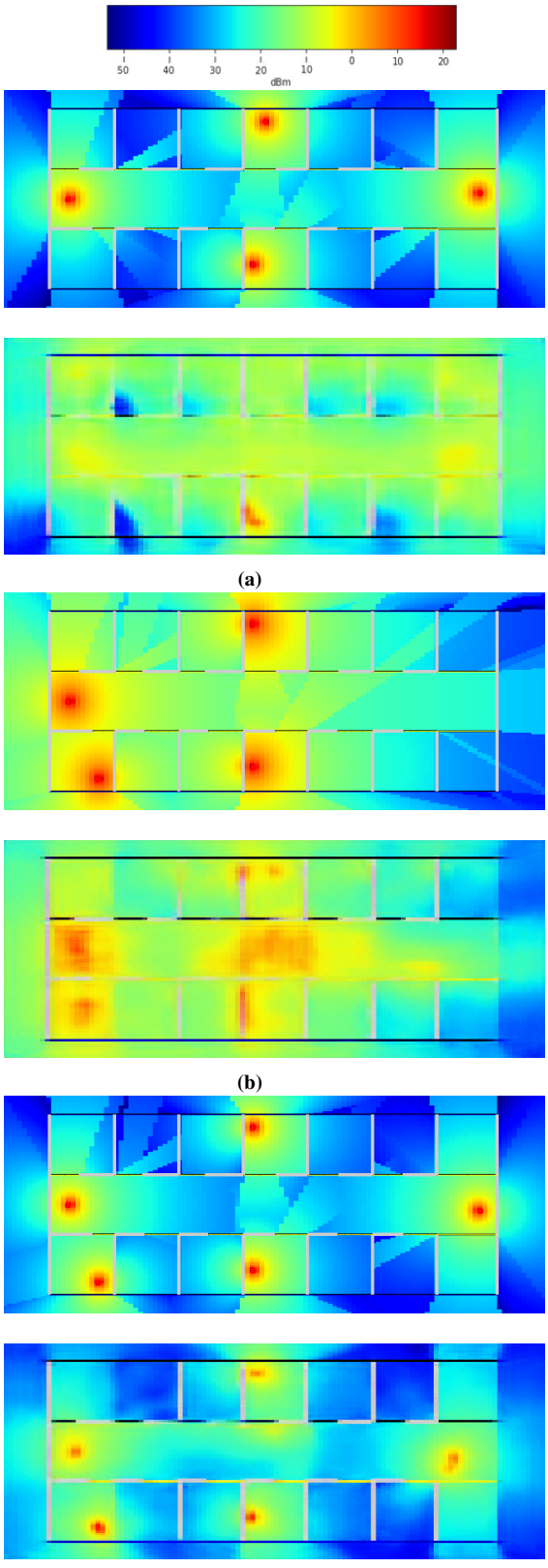

(a)

(b)

(c)

Fig. 8: Reconstructed maps (rows 2, 4 and 6) and its corresponding original exposure maps (rows 1, 3 and 5) when (a) 15, (b) 50, (c) 90 pixels used as sensor measurements at random locations.

IV. Conclusion

This paper proposed an RF-EMF exposure map estimation method, called EME-Net, based on the U-net architecture, for indoor wireless networks. Using a deep convolutional architecture, the proposed EME-Net was designed to predict the RF-EMF exposure maps accurately. The results illustrated that, using the developed model, it is possible to reconstruct the exposure maps accurately with fewer measurements at random locations, i.e., with less than 1% of the area of the reference map. The model learns the complex indoor radio environment propagation features through a training process and utilizes them to make accurate predictions rather than making unreliable or tendentious signal propagation assumptions. The architecture model could be extended or developed to cover outdoor or more sophisticated environments.

V. Acknowledgement

This project was partially supported by the Beyond5G project, funded by the French government as part of the economic recovery plan and the future investment program. This research work is done at IRCICA, USR CNRS 3380,Lille. Special Thanks to Métropole Européenne de Lille (MEL) for supporting this PhD project.

References

[1] M. H. Repacholi, E. v. Deventer, P. Ravazzani, W. H. Organization *et al.*, "Base stations and wireless networks: exposures and health consequences: proceedings, international workshop on base stations and wireless networks: Exposures and health consequences, switzerland, geneva, june 15-16, 2005," 2007.

[2] E. Chiaramello, M. Parazzini, S. Fiocchi, M. Bonato, P. Ravazzani, and J. Wiart, "Stochastic exposure assessment to 4g lte femtocell in indoor environments," in *2018 2nd URSI Atlantic Radio Science Meeting (AT-RASC)*. IEEE, 2018, pp. 1–4.

[3] A. N. des Fréquences, "Analyse des résultats de mesures d'exposition du public aux ondes électromagnétiques réalisées en 2017 dans le cadre du dispositif national desurveillance." Fact Sheet N°282, 2018, https://www.anfr.fr/fileadmin/mediatheque/documents/expace/20180919-Analyse-mesures-2017.pdf, Last accessed on 2021-04-06.

[4] X. Han, L. Xue, F. Shao, and Y. Xu, "A power spectrum maps estimation algorithm based on generative adversarial networks for underlay cognitive radio networks," *Sensors*, vol. 20, no. 1, p. 311, 2020.

[5] I. Goodfellow, J. Pouget-Abadie, M. Mirza, B. Xu, D. Warde-Farley, S. Ozair, A. Courville, and Y. Bengio, "Generative adversarial networks," *Communications of the ACM*, vol. 63, no. 11, pp. 139–144, 2020.

[6] I. J. Goodfellow, J. Pouget-Abadie, M. Mirza, B. Xu, D. Warde-Farley, S. Ozair, A. Courville, and Y. Bengio, "Generative adversarial networks," *arXiv preprint arXiv:1406.2661*, 2014.

[7] O. Ronneberger, P. Fischer, and T. Brox, "U-net: Convolutional networks for biomedical image segmentation," *CoRR*, vol. abs/1505.04597, 2015. [Online]. Available: http://arxiv.org/abs/1505.04597

[8] Z. Wang, A. Bovik, H. Sheikh, and E. Simoncelli, "Image quality assessment: from error visibility to structural similarity," *IEEE Transactions on Image Processing*, vol. 13, no. 4, pp. 600–612, 2004.

[9] J. Meinilä, T. Jämsä, P. Kyösti, D. Laselva, H. El-Sallabi, J. Salo, and D. B. Schneider, "Ist-2003-507581 winner d5. 2 determination of propagation scenarios."

[10] N. Amiot, M. Laaraiedh, and B. Uguen, "Pylayers: An open source dynamic simulator for indoor propagation and localization," in *2013 IEEE International Conference on Communications Workshops (ICC)*. IEEE, 2013, pp. 84–88.

[11] M. Kacou, V. Guillet, G. E. Zein, and G. Zaharia, "A multi-wall and multi-frequency home environment path loss characterization and modeling," in *12th European Conference on Antennas and Propagation (EuCAP 2018)*, 2018, pp. 1–5.